Bulk Mediated Surface Diffusion: Non Markovian Desorption with Finite First Moment

Jorge A. Revelli,[1,*] Carlos. E. Budde,[1,†] Domingo Prato,[1,‡] and Horacio S. Wio[2,3,§]

[1] *Facultad de Matemáticas, Astronomía y Física, Universidad Nacional de Córdoba 5000 Córdoba, Argentina;*

[2] *Instituto de Física de Cantabria, E-39005 Santander, Spain*

[3] *Grupo de Física Estadística, Centro Atómico Bariloche and Instituto Balseiro, 8400 San Carlos de Bariloche, Argentina*

Abstract

Here we address a fundamental issue in surface physics: the dynamics of adsorbed molecules. We study this problem when the particle's desorption is characterized by a non Markovian process, while the particle's adsorption and its motion in the bulk are governed by a Markovian dynamics. We study the diffusion of particles in a semi-infinite cubic lattice, and focus on the effective diffusion process at the interface $z = 1$. We calculate analytically the conditional probability to find the particle on the $z = 1$ plane as well as the surface dispersion as functions of time. The comparison of these results with Monte Carlo simulations show an excellent agreement.

PACS numbers: 46.65.+g, 05.40.FW., 05.10.Ln., 02.50.Eg.

[*] Electronic address: jorgerevelli@yahoo.com

[†] Electronic address: budde@famaf.unc.edu.ar

[‡] Electronic address: prato@famaf.unc.edu.ar

[§] Electronic address: wio@ifca.unican.es

I. INTRODUCTION

The mechanism called *bulk-mediated surface diffusion* typically arises at interfaces separating a liquid bulk phase and a second phase which may be either solid, liquid, or gaseous. Whenever the adsorbed species is soluble in the liquid bulk, adsorption-desorption processes occur continuously. These processes generate surface displacement because desorbed molecules undergo Fickian diffusion in the liquid's bulk, and are latter re-adsorbed elsewhere. When this process is repeated many times, an effective diffusion results for the molecules on the surface. The importance of bulk-surface exchange in relaxing homogeneous surface density perturbations is experimentally well established [1, 2, 3, 4, 5]. Adsorption at the solid-liquid interfaces arises, for instance, in many biological contexts involving protein deposition [6, 7, 8], in solutions or melts of synthetic macromolecules [9, 10, 11, 12], in colloidal dispersions [13], and in the manufacture of self-assembly mono- and multi-layers [14, 15, 16, 17].

Usually the studies performed in this type of systems are done within the framework of a Master Equation scheme [18, 19], where the particle's motion through the bulk and the adsorption-desorption processes are Markovian. In two recent papers [20, 21] we have shown the most important features of these phenomena. Non Markovian diffusion processes have been used in order to modelling a great diversity of phenomena some of the most relevant are: anomalous charge transport in amorphous materials [22], diffusion of particles with internal states [23], chromatography [18], dielectric relaxation due to defect diffusion [24].

We address one of the fundamental issues in surface physics: the dynamics of adsorbed molecules. We study this problem when the particle's desorption is characterized by a non Markovian process, while the particle's adsorption and its motion in the bulk are governed by a Markovian dynamics. We analyze the diffusion of particles in a semi-infinite cubic lattice, and focus on the effective diffusion process at the interface $z = 1$. We calculate analytically the conditional probability to find the particle on the $z = 1$ plane as well as the surface dispersion as functions of time, and test those results comparing with Monte Carlo simulations. When non Markovian processes are present Generalize Master Equations are involved, these equations being characterized by a "memory kernel" that is related univocally with a Continuous Time Random Walk (CTRW) scheme [25].

Non Markovian desorption has been introduced in many fields of natural science de-

scribing transport processes in chemical reactions [26], re-emission when surfaces contains "deep traps" [27], capture and re-emission from surfaces that contain sites with many internal states such the "ladder trapping model" [28], proteins with active sites deep inside its matrix [29] , etc.

The main goal of this work is to get information about the influence of a non Markovian desorption dynamics on the effective diffusion process at the interface $z = 1$, and in this way to develop some criteria for looking for non Markovian desorption effects in experimental situations. For that purpose we calculate analytically the temporal evolution of the variance ($\langle r^2(t)\rangle_{plane}$) and the conditional probability of being on the surface at time t since the particle arrived there at $t = 0$ ($P(x, y, z = 1; t|0, 0, 1, t = 0)$), that we indicate by $P(z = 1, t)$.

When $\psi(t)$, the waiting time density for desorption defined in the CTRW scheme, has a **finite first moment** we have been able to establish the long time asymptotic behavior for $\langle r^2(t)\rangle_{plane}$ and $P(z = 1, t)$ for **any** non-Markovian desorption. This behavior is the same as the Markovian one and only depends on the first moment of $\psi(t)$. We also analyzed the behavior associated to two different families of desorption waiting time densities. For the first one we have observed two regions, called *strong* and *weak adsorption* regime (to be defined later). In the strong adsorption limit we observe a transient regime, where the temporal evolution is characterized by damped oscillations (its frequency not depending on the degree of departure from Markovian behavior), and a Markovian asymptotic one. The oscillatory effects disappear in the weak adsorption region. For the second kind of desorption dynamics, a transient regime with a non-monotonic behavior for the slope of the variance emerges, the asymptotic behavior being again Markovian like.

The organization of the paper is as follows. In the next Section we formally present the model, supported by a Generalized Master Equation which describe the particle's dynamics through the bulk and the adsorption-desorption dynamics at the surface. We devote Section III to present and discuss the time dependence of $\langle r^2(t)\rangle_{plane}$ and $P(z = 1, t)$ for two families of specific memory kernels, and compare the analytical results with Monte Carlo simulations in the first case, and discuss the general characteristics in the second. In Section IV we study the asymptotic behavior of the aforementioned magnitudes, in the asymptotic long time limit. In the last Section we discuss the results and present some conclusions.

II. THE ADSORPTION-DESORPTION MODEL

Let us start with the problem of a particle making a random walk in a semi-infinite cubic lattice (with a lattice constant equal to one). The position of the walker is defined by a vector $\vec{r}$ whose components are denoted by a set of integer numbers n, m, l corresponding to the directions x, y and z respectively. The probability that the walker is at (n, m, l) for time t given it was at $(0, 0, l_0)$ at $t = 0$, $P(n, m, l; t|0, 0, l_0, t = 0) = P(n, m, l; t)$, satisfies the following Generalized Master Equation

$$\begin{aligned}
\dot{P}(n,m,1;t) &= \gamma P(n,m,2;t) - \int_0^t dt'\, K(t')P(n,m,1;t-t'), && \text{for } l=1 \\
\dot{P}(n,m,2;t) &= \int_0^t dt'\, K(t')P(n,m,1;t-t') + \gamma P(n,m,3;t) - \gamma P(n,m,2;t) \\
&\quad +\alpha[P(n-1,m,2;t) + P(n+1,m,2;t) - 2P(n,m,2;t)] \\
&\quad +\beta[P(n,m-1,2;t) + P(n,m+1,2;t) - 2P(n,m,2;t)], && \text{for } l=2 \\
\dot{P}(n,m,l;t) &= \alpha[P(n-1,m,l;t) + P(n+1,m,l;t) - 2P(n,m,l;t)] \\
&\quad +\beta[P(n,m-1,l;t) + P(n,m+1,l;t) - 2P(n,m,l;t)] \\
&\quad +\gamma[P(n,m,l+1;t) + P(n,m,l-1;t) - 2P(n,m,l;t)], && \text{for } l \geq 3, \quad (1)
\end{aligned}$$

α, β and γ are the transition probabilities per unit time through the bulk in the x, y and z directions respectively and $K(t)$ represents the memory kernel at all sites $(n, m, l = 1)$ and $(n, m, l = 2)$. The form of these equations is similar to those indicated in [20, 21], with the desorption parameter δ replaced by the kernel $K(t)$.

In order to solve the above equations we follow the same procedure as in [20, 21], taking the Fourier transform with respect to the x and y variables and the Laplace transform with respect to the time t in the above equations, we obtain

$$\begin{aligned}
sG(k_x,k_y,1;s) - P(k_x,k_y,1,t=0) &= \gamma G(k_x,k_y,2;s) - K(s)G(k_x,k_y,1;s), \qquad l=1 \\
sG(k_x,k_y,2;s) - P(k_x,k_y,2,t=0) &= A(k_x,k_y)G(k_x,k_y,2;s) + K(s)G(k_x,k_y,1;s) + \\
&\quad \gamma G(k_x,k_y,3;s) - 2\gamma G(k_x,k_y,2;s), \qquad l=2 \\
sG(k_x,k_y,l;s) - P(k_x,k_y,l,t=0) &= A(k_x,k_y)G(k_x,k_y,l;s) + \\
&\quad \gamma[G(k_x,k_y,l-1;s) + \\
&\quad G(k_x,k_y,l+1;s) - 2G(k_x,k_y,l;s)]. \qquad l \geq 3 \quad (2)
\end{aligned}$$

We have used the following definitions [20, 21]

$$
\begin{aligned}
G(k_x, k_y, l; s) &= G(k_x, k_y, l; s|0, 0, l_0; t = 0) \\
&= \int_0^{\infty} e^{-st} \sum_{n,m,-\infty}^{\infty} e^{i(k_x n + k_y m)} P(n, m, l; t) dt \\
&= L[\sum_{n,m,-\infty}^{\infty} e^{i(k_x n + k_y m)} P(n, m, l; t)], \qquad (3)
\end{aligned}
$$

where L indicates the Laplace transform of the quantity within the brackets, and [20, 21]

$$A(k_x, k_y) = 2\alpha[\cos(k_x) - 1] + 2\beta[\cos(k_y) - 1]. \qquad (4)$$

Equation (2) may be expressed in matrix form as

$$[s\tilde{I} - \tilde{H}]\tilde{G} = \tilde{I}, \qquad (5)$$

where the square matrix $\tilde{G}$ has components

$$\tilde{G}_{ll_0} = [G[k_x, k_y, l; s|0, 0, l_0; t = 0]]. \qquad (6)$$

$\tilde{I}$ is the identity matrix and $\tilde{H}$ is a three-diagonal matrix with the following form

$$\tilde{H} = \begin{pmatrix} -K(s) & \gamma & 0 & 0 & 0 & \cdots \\ K(s) & C & \gamma & 0 & 0 & \cdots \\ 0 & \gamma & C & \gamma & 0 & \cdots \\ 0 & 0 & \gamma & C & \gamma & \cdots \\ . & . & . & . & . & \cdots \end{pmatrix},$$

where C is defined as

$$C = -2\gamma + A(k_x, k_y). \qquad (7)$$

Above equations for $G(k_x, k_y, l; s)$ are similar to Eq.(2) and Eq.(5) in [20] with $K(s)$ replacing δ. Therefore, all results obtained in that paper remains valid for non-Markovian dynamic when δ is replaced by $K(s)$ in the Laplace domain.

The expression for the Laplace transform of the variance ($\langle r^2(s)\rangle_{plane}$) became

$$L[\langle r^2(t)\rangle_{plane}] = \langle r^2(s)\rangle_{plane} = \frac{N(s)}{D(s)}, \qquad (8)$$

with

$$N(s) = [4K(s)\gamma(\alpha+\beta)] \left[2\gamma^3 - s^2(\sqrt{s(4\gamma+s)} - s) - 3\gamma^2(\sqrt{s(4\gamma+s)} - 3u) - 2\gamma s(2\sqrt{s(4\gamma+s)} - 3s)\right], \tag{9}$$

$$D(s) = \sqrt{s(4\gamma+s)} \left[\gamma s(2\gamma + s - \sqrt{s(4\gamma+s)}) + K(s)(\gamma(\sqrt{s(4\gamma+s)} - 3s) + s(\sqrt{s(4\gamma+s)} - s))\right]^2. \tag{10}$$

The Laplace transform of $P(z=1,s)$, the conditional probability of being in the surface, is

$$L[P(z=1,t)] = P(z=1,s) = \left[\gamma(2\gamma + s - \sqrt{s(4\gamma+s)}\right] \left[\gamma s(2\gamma + s - \sqrt{s(4\gamma+s)}) + K(s)(\gamma(\sqrt{s(4\gamma+s)} - 3s) + s(\sqrt{s(4\gamma+s)} - s))\right]^{-1}. \tag{11}$$

Finally we want to point out that the relation between $\psi(t)$, the waiting time density for the desorption processes defined in the CTRW scheme, and the memory kernel of Eq. (1) [25] in the Laplace domain is given by

$$K(s) = \frac{s\psi(s)}{(1-\psi(s))}. \tag{12}$$

III. ANALYTICAL RESULTS AND MONTE CARLO SIMULATIONS

Here we show the results obtained analytically and compare them with Monte Carlo simulations. In all cases we have fixed the parameters: $\alpha = \beta = \gamma = 1$. The simulations results were obtained averaging over 2×10^6 realizations.

To describe the desorption dynamics from the surface we have chosen two families of waiting time densities ($\psi(t)$). The first of them was introduced by Scher and Lax [22] to describe the frequency dependence of the electric conductivity in disordered solids when transport is due to impurity hopping. It has been extensively exploited in modelling non Markovian cases that emerge when an average over transition rates (disorder) is taking into account [22] and [25]. The reason of its wide use are its versatile functional form and its simplicity which allows to take into account a controllable spread of transition rates [22]. When only one transition rate is present the Markovian description is reobtained (the

memory kernel is a Dirac delta function) and when the spread is very wide, steps occur at fixed regular intervals of time (see below). The adopted function (see also [30]) is

$$\psi(t) = \theta a \frac{(\theta a t)^{(a-1)}}{\Gamma(a)} e^{-\theta a t}, \tag{13}$$

where a is a positive integer and $\Gamma(a)$ is the Gamma or Factorial Function. It is worth remarking here two important facts about this family of functions. First, as can be seen from the Eq. (13), there are two parameters which characterized the function. The parameter a, called *markovianicity parameter*, defines the degree of function's departure from the Markovian behavior ($a = 1$ corresponds to the Markovian case; $a \neq 1$ to the non-Markovian case), while the parameter θ is the "average desorption's rate". Second, as shown in [30], the mean value of these waiting time densities is

$$\langle t \rangle = \int_0^\infty t \;\; \psi(t) \;\; dt = \theta^{-1}, \tag{14}$$

showing that the "average desorption's time" does not depends on the parameter a. For the form of this family of functions, see Fig. 1 in [30].

In Figs. 1 and 2 we present the temporal evolution for the conditional probability ($P(z = 1, t)$) for the Markovian and two non Markovian cases (two different values of a) with the same value of θ. From these figures we can observe two temporal regions: a transient one which ranges from $t = 0$ to $t \approx 1000$ and an asymptotic region ($t > 1000$) where the behavior approaches that of the Markovian case. It is important to remark the existence of damped oscillations in the transient region for the non Markovian case. This oscillatory behavior is due to the waiting time density functions used as will be explained later.

In Figs. 3 and 4 we depict the results for the variance $\langle r^2(t) \rangle_{plane}$, for both the Markovian and the two different non Markovian cases ($a = 75$ and $a = 100$). We can observe two important features. The first one is that the variance in the non Markovian regime shows a delay in the beginning of the spreading. The second feature is that the system presents an oscillatory-like behavior, with the oscillations attenuating as the time grows. This fact is still more apparent in the insert of the figures where we show the temporal evolution of the *spreading velocity* (V_{Spread}). It is worth remarking here that oscillations only appears in the non Markovian case with $a \gg 1$ and are due to the particular behavior of the family of waiting time density defined by Eq. (13). As it is known, this function goes to a Dirac delta function as the markovianicity parameter $a \to \infty$ ($\psi(t) \Rightarrow \delta(t - \theta^{-1})$), implying a

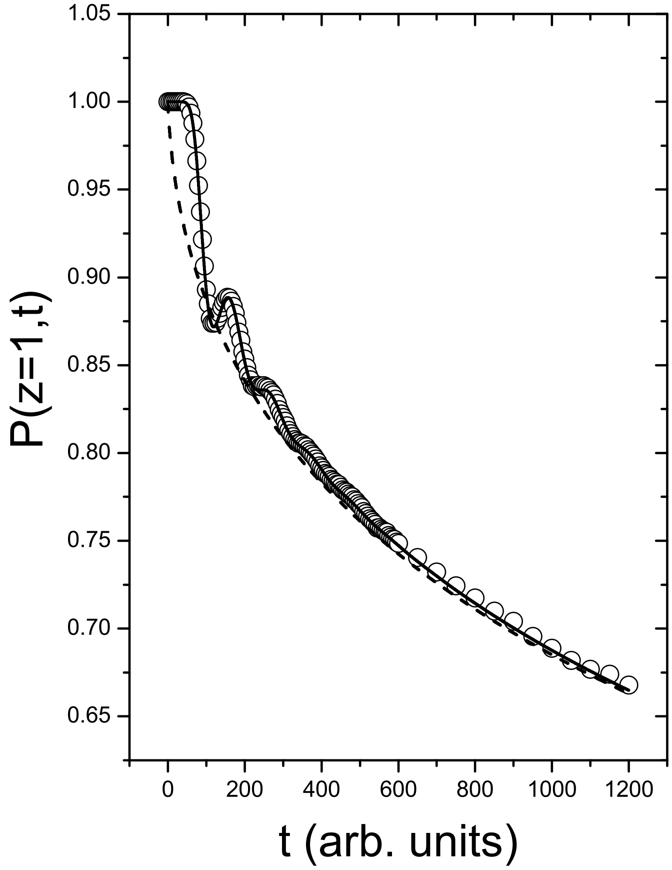

FIG. 1: Temporal evolution of the $P(z = 1, t)$. We have represented the case for $\theta = 0.01$. Dot line depicts Markovian evolution, meanwhile continuous line and open circles (which correspond to Monte Carlo simulations) represent the non Markovian case for $a = 20$

.

periodic-like behavior. This "periodicity" explains the oscillatory behavior of $P(z = 1, t)$ and $\langle r^2(t)\rangle_{plane}$. Also the figures show an excellent agreement between the theoretical and Monte Carlo simulation results.

We remark here that we can distinguish two region defined by the ratio θ/γ. The *strong adsorption region* characterized by $\frac{\theta}{\gamma} << 1$ where the non Markovian character shows important differences respect to the Markovian case in the transient temporal regime and the *weak adsorption region* ($\frac{\theta}{\gamma} > 1$) where these differences disappear.

Another worth remarking point from these figures is that ω, the frequency in the oscillation, remains unperturbed due to the fact that all desorption waiting time densities used

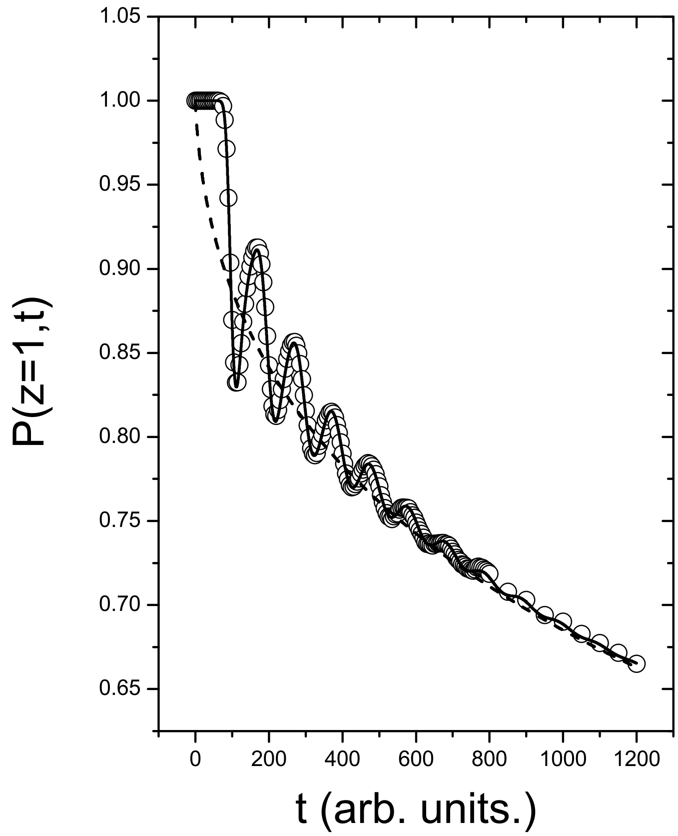

FIG. 2: Temporal evolution of the $P(z = 1, t)$. We have represented the case for $\theta = 0.01$. Dot line depicts Markovian evolution, meanwhile continuous line and open circles (which correspond to Monte Carlo simulations) represent the non Markovian case for $a = 75$

.

have the same "average desorption's time". This aspect becomes apparent in Fig. 5.

The second class of desorption dynamics that we consider in this work corresponds to the so called "direct-access multi-trapping process" [28]. Such an approach was proposed in order to describe in a phenomenological manner the transport of excited charge carriers across amorphous material [31, 32], or the motion of intersticial in metals [33], etc. When the walker arrives at a surface site this model considers transitions to and from $(N - 1)$ internal states, both with probability λ per unit time, before it desorbs to the bulk with probability δ. The resulting desorption probability waiting time density in Laplace domain

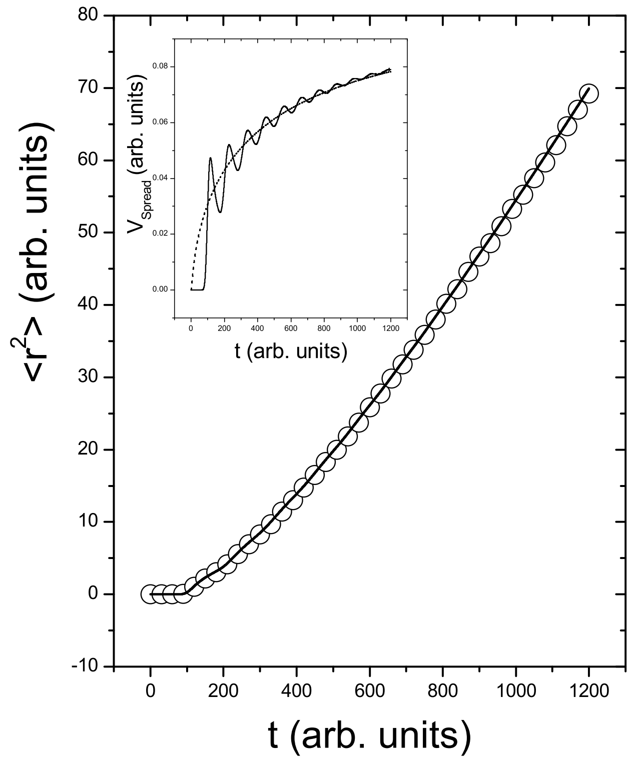

FIG. 3: Temporal evolution of the $\langle r^2(t)\rangle_{plane}$. We have taken $\theta = 0.01$. The solid line and open circles (which correspond to Monte Carlo simulations) depict the non Markovian case with $a = 75$. In the insert we can see the V_{Spread} vs. t for this case (solid line) and the Markovian evolution (dot line)

is

$$\psi(s) = \frac{\delta}{\delta + s(1 + \frac{\lambda(N-1)}{s+\lambda})} \tag{15}$$

and the "average desorption's rate" in this case is $\langle t\rangle = \frac{N}{\delta}$. For a detailed analysis of this model and derivation of Eq. (15) see Ref. [28]. In Figs. 6 and 7 we depict the results for the variance $\langle r^2(t)\rangle_{plane}$ for two different non Markovian cases ($N = 2$ and $N = 10$ respectively). We also show the Markovian behavior with the same average time for each case ($\langle t\rangle = 2$ for $N = 2$ and $\langle t\rangle = 10$ for $N = 10$). We can observe that the temporal evolution of the variance in the non Markovian case shows a transient regime characterized by the slope's non-monotonic behavior, which increases with N. This fact is still more apparent in the

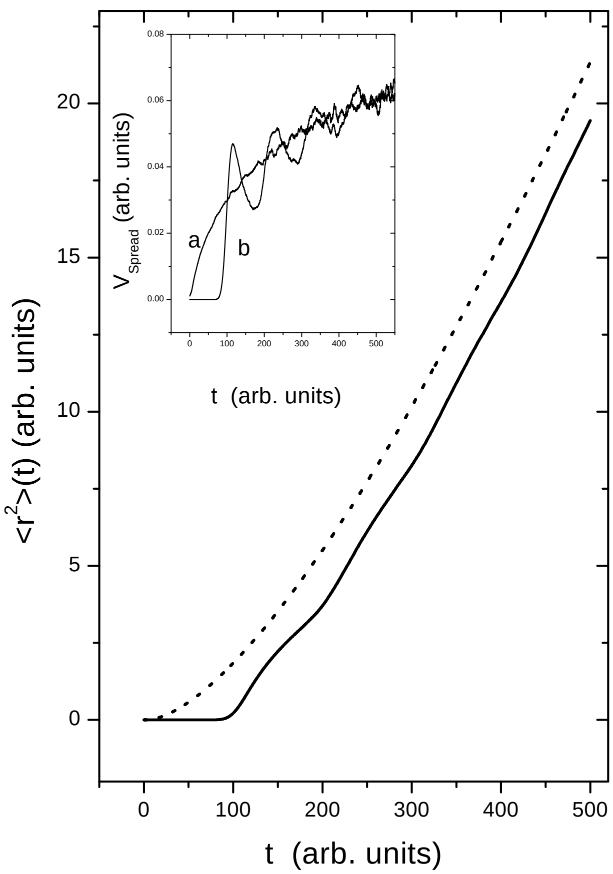

FIG. 4: Temporal evolution of the variance $\langle r^2(t)\rangle_{plane}$. We have represented two cases. Dot line represents the Markovian case and the continuous line depict the non Markovian ($a = 100$) for $\theta = 0.01$. In the insert the curve denoted by a represents the Markovian case; the b curve represents the non Markovian one.

insert of the figures where we show the temporal evolution of the *spreading velocity* (V_{Spread}).

IV. ASYMPTOTIC BEHAVIOR

The asymptotic behavior for large t of $\langle r^2(t)\rangle_{plane}$ and $P(z = 1, t)$ can be obtained analyzing the limit $s \ll 1$. We assume that $\psi(t)$, the waiting time density for desorption, has a **finite first moment** $\langle t\rangle$ which means that $\psi(t) \sim 1 - \langle t\rangle s$ when $s \ll 1$ and consequently

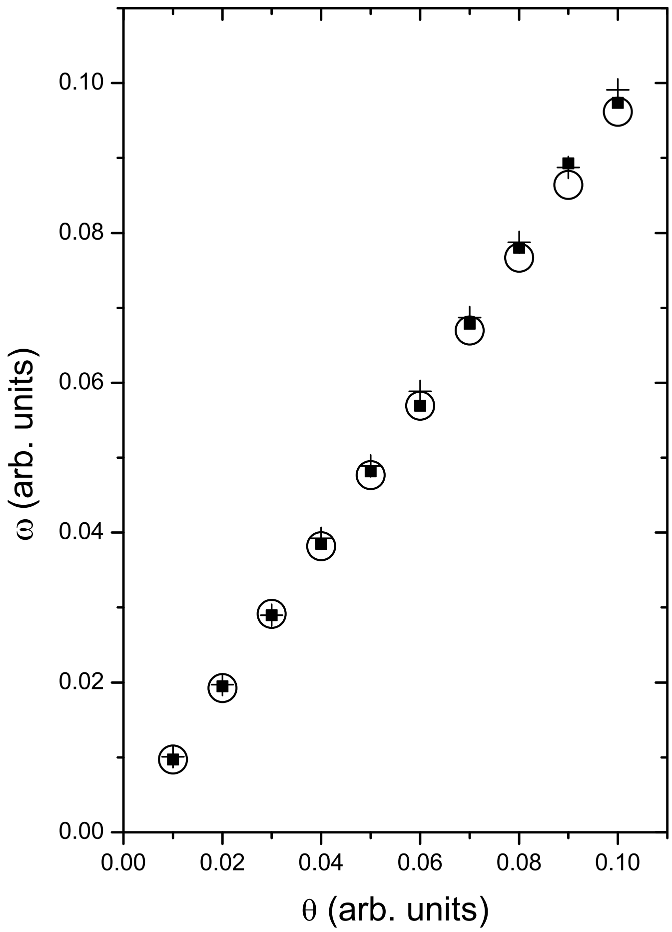

FIG. 5: ω vs. θ. Open circles represents $a = 100$, squares $a = 200$ and cruxes $a = 500$.

$K(s) \sim 1/\langle t \rangle$ in this limit. From Eqs. (8), (9), (10) and (11) we obtain

$$\langle r^2(t) \rangle_{plane} \sim \frac{\sqrt{\gamma}(\alpha + \beta)\langle t \rangle}{2s^{\frac{3}{2}}}, \tag{16}$$

$$P(z = 1, t) \sim \frac{\sqrt{\gamma}\langle t \rangle}{s^{\frac{1}{2}}}. \tag{17}$$

Exploiting Tauberian theorems [25], the behavior for large t can be obtained resulting in

$$\langle r^2(t) \rangle_{plane} \sim \frac{\sqrt{\gamma}(\alpha + \beta)\langle t \rangle}{2\Gamma[3/2]} \quad t^{\frac{1}{2}}, \tag{18}$$

$$P(z = 1, t) \sim \frac{\sqrt{\gamma}\langle t \rangle}{\Gamma[1/2]} \quad t^{-\frac{1}{2}}. \tag{19}$$

Equations (18) and (19) represent the behavior of $\langle r^2(t) \rangle_{plane}$ and $P(z = 1, t)$ for **any** non-Markovian desorption for large values of time. This behavior is the same as the Markovian

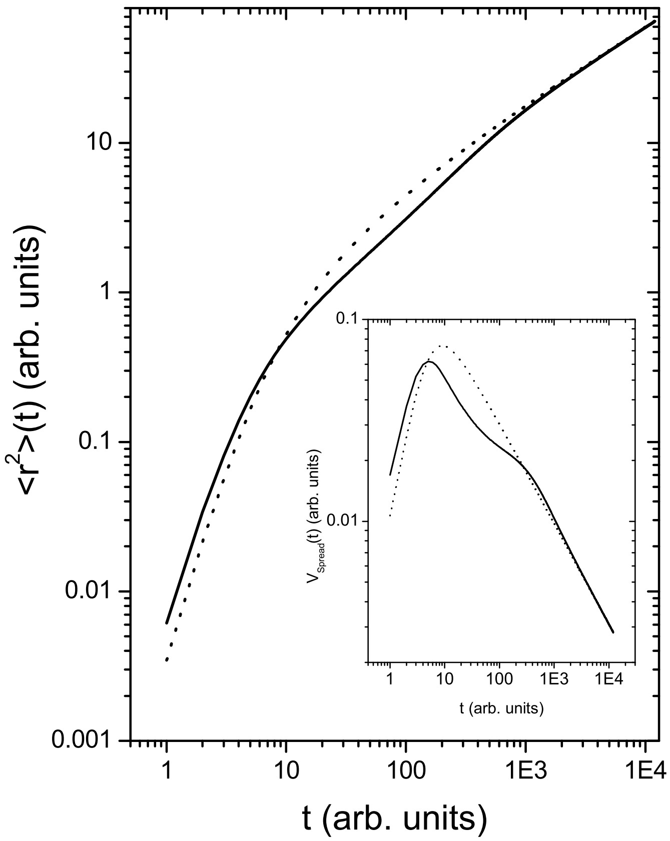

FIG. 6: Temporal evolution of the $\langle r^2(t)\rangle_{plane}$. The solid line depicts the non Markovian case with $N = 2$, $\delta = 1$ and $\lambda = 0.01$ and the dot line the Markovian one. In the insert we can see the V_{Spread} vs. t for this case (solid line) and the Markovian evolution (dot line)

one and only depends on the first moment of $\psi(t)$. It is important to remark that the only assumption was that $\psi(t)$, the waiting time density for desorption, has a finite first moment $\langle t\rangle$.

V. CONCLUSIONS

We have studied here the evolution of particles diffusing on a surface. The diffusion have been performed across the bulk surrounding the surface, this phenomenon being called *bulk mediated surface diffusion*[20, 21]. Usually the proposed models are based on Markovian desorption processes. The main feature of this work was to present an analytical model for non Markovian desorption from the surface. The bulk that surrounds this surface was

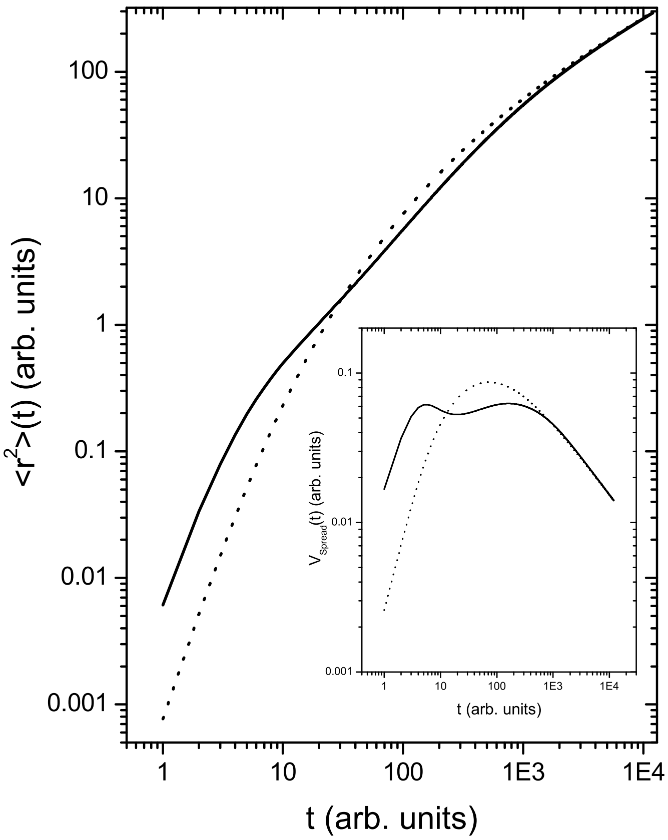

FIG. 7: Temporal evolution of the $\langle r^2(t)\rangle_{plane}$. The same parameters as in Fig. 6 but with $N = 10$

considered to be semi-infinite and that the particles undergo a Markovian motion on them.

We observed the influence of the non Markovian desorption dynamic on the effective diffusion process at the interface $z = 1$ by calculating analytically, in the Laplace domain, the temporal evolutions of the variance ($\langle r^2(t)\rangle_{plane}$) and the conditional probability of being on the surface at time t since the particle arrived there at $t = 0$ ($P(z = 1, t)$). When the waiting time density for desorption has a **finite first moment** we have established the behavior of the above magnitudes for **any** non-Markovian desorption for large values of time. This behavior is the same as the Markovian one and only depends on the first moment of $\psi(t)$.

We have chosen two families of non-Markovian desorption waiting time densities and tested the analytical results for $\langle r^2(t)\rangle_{plane}$ and $P(z = 1, t)$ by comparison with Monte Carlo simulations, obtaining an excellent agreement. For the first desorption waiting time density we can establish two regions based on the ratio θ/γ, calling them *strong adsorption* (this

occurs when $\theta/\gamma << 1$) and *weak adsorption* (when $\theta/\gamma \geq 1$). In the strong adsorption limit we can observe a transient regime and a stationary one. The main feature in the transient regime is that the temporal evolution is characterized by damped oscillations whose frequencies are in direct relation to θ, the average desorption rate. It is worth remarking here that the frequency does not depend on the markovianicity parameter. The effect of this parameter appears on the amplitude of the oscillations which disappear in the weak adsorption region. For the second kind of desorption dynamics we found a transient regime with an emerging non-monotonic behavior for the slope's variance. In the asymptotic regime, the conditional probability of the non Markovian system tends to the Markovian one as is expected from the analytical results obtained in Section IV. In a recent paper [34] we have shown that, when we consider **finite** or **infinite biased** systems, and desorption waiting time densities with finite first moment, the variance growths linearly with time in the asymptotic regime.

Finally, it is worth here remarking an important aspect of the present approach. We have shown through the above results that the behavior of $\langle r^2(t)\rangle_{plane}$ and $P(z=1,t)$ results to be strongly dependent on the desorption mechanism. As the effective dispersion and the percentage of particles that remain on the plane $z=1$ are measurable magnitudes [19] they could be used to investigate the characteristic and get information about the fundamental parameters of the desorption processes.

Acknowledgments: HSW acknowledges the partial support from ANPCyT, Argentine, and thanks the European Commission for the award of a *Marie Curie Chair*.

[1] V. G. Levich, *Physiochemical Hydrodynamics* (Prentice-Hall, NJ, 1962), 2nd ed.

[2] E. H. Lucassen-Reynders, J. Lucassen, Adv. Colloid Interface Sci **2** 347 (1969).

[3] E. H. Lucassen-Reynders, et al., Adv. Chem. Scr. **144**, 272 (1975).

[4] C.T. Shibata, A. M Lenhof, J. Colloid Interface Sci. **148**, 469 (1992), **148**, 485 (1992).

[5] S-Y. Lin K. McKeigue, C. Maldarelli, AIChE J. **36** (12), 1785 (1990).

[6] L. Vroman, A. L. Adams, J. Colloid Interface Sci. **111** (1986) 391.

[7] J.L. Brash, P. ten Hove, Thromb Haemostasis **51** (1984) 326.

[8] R.J. Rapoza, T.A. Horbett, J. Colloid Interface Sci. **136** (1990) 480.

[9] S.J. Alexander, Phys. France **38** (1977) 983.

[10] P.G. de Gennes, J. Phys. **37** (1976) 1445,

[11] P.G. de Gennes, Adv. Colloid Interface Sci. **27** (1987) 189.

[12] J.F. Douglas, H.E. Johnson, S. Granick, Science **262** (1993) 2010.

[13] B.L. Carvalho, P. Tong, J.S. Huang, T.A. Witten, L.J. Fetters, Macromolecules **26** (1993) 4632,

[14] J.H. Clint, *Surfactant Aggregation* (Blackie, Glasgow and London, 1992).

[15] L. Netzer, J. Sagiv, J. Am. Chem. Soc. **105** (1983) 674.

[16] E.B. Troughton, C.D. Bain, G.M. Whitesides, Langmuir **4** (1987) 365.

[17] Y.L. Chen, S. Chen, C. Frank, I. Israelachvili, J. Colloid Interface Sci. **153** (1992) 244.

[18] N.G. van Kampen, *Stochastic Processes in Physics and Chemistry*, 2nd ed. (North Holland, Amsterdam, 1993).

[19] O. Bychuk, B. O'Shaughnessy, Phys. Rev. Lett. **74**, 10, 1795 (1995).

[20] J.A. Revelli, C.E. Budde, D. Prato, H.S. Wio, Eur. Phys. J. B **36**, 245 (2003).

[21] J.A. Revelli, C.E. Budde, D. Prato, H.S. Wio, Eur. Phys. J. B **37**, 205 (2004).

[22] H. Scher, M. Lax, Phys. Rev. B, **7**, 4491; and 4502 (1973).

[23] G.H. Weiss, R.J. Rubin, Adv. Chem. Phys. **52**, 363 (1983).

[24] J. T. Bendler, M. F. Shlesinger, in *The Wonderful World of Stochastics*, M. F. Shlesinger, G. H. Weiss, eds. (Elsevier, Amsterdam,1985).

[25] E.W. Montroll, B.J. West, in *Fluctuation Phenomena*, E.W. Montroll, J.L. Lebowitz, eds. (North Holland, Amsterdam, 1979).

[26] W. P. Helman, K. Funabashi, J. Chem. Phys. **71**, 2458 (1979).

[27] M. A. Re, C. E. Budde, Phys. Rev. E. **61**, 1110 (2000).

[28] J. W. Haus, K. W. Kehr, Phys. Rep. **150**, 265 (1987).

[29] W. Nadler, D. L. Stein, J. Chem. Phys. **104**, 1918 (1996).

[30] J.A. Revelli, C.E. Budde, H.S. Wio, Phys. Lett. A **306**, 104 (2002).

[31] G. Pfister, H. Scher, Adv. Phys. **27**, 74 (1978).

[32] J. Noolandi, Phys. Rev. B **16**, 4466 (1977)

[33] D. Richter, T. Springer, Phys. Rev. **B18**, 126 (1978)

[34] J.A. Revelli, C.E. Budde, D. Prato, H.S. Wio, *Bulk Mediated Surface Diffusion: The Probability of Return to the Plane*, to be submitted to Europ. Phys. J. B.